An anteroposterior wave of vascular inhibitor downregulation signals aortae fusion along the embryonic midline axis

Robert J. Garriock, Catherine Czeisler, Yasuo Ishii, Alicia M. Navetta and Takashi Mikawa*

SUMMARY

Paracrine signals, both positive and negative, regulate the positioning and remodeling of embryonic blood vessels. In the embryos of mammals and birds, the first major remodeling event is the fusion of bilateral dorsal aortae at the midline to form the dorsal aorta. Although the original bilaterality of the dorsal aortae occurs as the result of inhibitory factors (antagonists of BMP signaling) secreted from the midline by the notochord, it is unknown how fusion is later signaled. Here, we report that dorsal aortae fusion is tightly regulated by a change in signaling by the notochord along the anteroposterior axis. During aortae fusion, the notochord ceases to exert its negative influence on vessel formation. This is achieved by a transcriptional downregulation of negative regulators while positive regulators are maintained at pre-fusion levels. In particular, Chordin, the most abundant BMP antagonist expressed in the notochord prior to fusion, undergoes a dramatic downregulation in an anterior to posterior wave. With inhibitory signals diminished and sustained expression of the positive factors SHH and VEGF at the midline, fusion of the dorsal aortae is signaled. These results demonstrate a novel mechanism by which major modifications of the vascular pattern can occur through modulation of vascular inhibitors without changes in the levels of positive vascular regulators.

KEY WORDS: Chordin, VEGF, SHH, Chick

INTRODUCTION

As the placement of major vessels in the embryo follows embryonic axial structures, it is presumed that paracrine signaling from these tissues shapes the positioning of vessels. Indeed, signals from the somites and notochord have profound influence on the early vascular pattern (Bressan et al., 2009; Cleaver and Krieg, 1998; Cleaver et al., 2000; Reese et al., 2004). The vast majority of identified paracrine factors promote vascular development. These vessel-promoting factors include vascular endothelial growth factor (VEGF) (Haigh, 2008; Senger et al., 1983), members of the hedgehog family (Dyer et al., 2001; Pola et al., 2001), fibroblast growth factors (FGFs) (Auguste et al., 2003; Gospodarowicz, 1976), bone morphogenetic proteins (BMP) (Nimmagadda et al., 2005; Reese et al., 2004), activins (Maeshima et al., 2004), TGFβ ligands acting through the ALK5 receptor (Goumans et al., 2002; Oh et al., 2000), angiopoietins (Davis et al., 1996; Suri et al., 1996) and apelin (Cox et al., 2006). In addition to vessel promoting factors, several secreted factors inhibit vascular development. These vessel inhibiting factors include semaphorin 3 members (Gaur et al., 2009; Gu et al., 2005; Serini et al., 2003), TGFβ ligands acting through the ALK1 receptor (Goumans et al., 2002; Heimark et al., 1986), angiopoietin 2 (Maisonpierre et al., 1997), chondromodulin (Hiraki et al., 1996; Hiraki et al., 1997), follistatins (Maeshima et al., 2004) and the BMP antagonists chordin, chordin-related 1 and noggin (Kane et al., 2008; Reese et al., 2004). Heavily vascularized regions of embryos typically occur

where positive vascular factors are expressed, and regions devoid of vessels typically occur where inhibitors are present. However, sites of positive vascular factor expression do not always dictate the placement of vessels, and it remains unclear how the embryonic vascular pattern is created and remodeled.

The molecular signals that position blood vessels in the vertebrate embryo are poorly understood, even for the most prominent embryonic vessel, the dorsal aorta (DA) or descending aorta. The DA is positioned exactly at the midline in the adult body plan. In the embryo and throughout adulthood, the DA is the main artery for circulation to tissues posterior to the heart. In amniotes (birds and mammals), DA development occurs first through the assembly of endothelial cells under the paraxial mesoderm. This forms bilateral vessels, the paired dorsal aortae, on either side of the midline (Pardanaud et al., 1987). Between the aortae is the midline avascular region, which is completely devoid of endothelial cells owing to the notochord expression of the BMP antagonists, *chordin* and *noggin* (Reese et al., 2004). After the second day of development, the paired dorsal aortae begin to fuse at the midline, eventually forming a single DA directly under the notochord. It is unclear how the DA forms under the notochord when the notochord is a source of inhibitory signals to endothelial cell development.

Although lower vertebrates do not form a DA from fusion of bilateral dorsal aortae, studies from frog and fish embryos have provided clues to how the DA is positioned. Endothelial cells of the fish and amphibian DA are recruited from free angioblasts in fish or from the posterior cardinal veins in amphibians through positive signals from the hypochord. The hypochord is a transitory chord of endodermally derived cells under the notochord, and is a source of positive vascular signals, including VEGF (Cleaver and Krieg, 1998; Hogan and Bautch, 2004). Conservation of developmental process suggests that positioning of the DA in amniotes might be

Cardiovascular Research Institute, University of California San Francisco, San Francisco, CA 94158, USA

*Author for correspondence (takashi.mikawa@ucsf.edu)

similar to fish and frog embryos, i.e. requiring a midline source of VEGF. However, amniote embryos do not form a hypochord and no prominent midline VEGF source occurs (Reese et al., 2004; Weinstein, 1999), suggesting an alternative mechanism to position the DA at the midline.

We show here that fusion of the dorsal aortae occurs from a developmental switch in signaling by the notochord. Prior to dorsal aortae fusion, the notochord is inhibitory to vessel formation, but at the time of fusion the notochord is no longer inhibitory. Through in vivo and in vitro experiments, we show that an anteroposterior wave of downregulation of vascular inhibitors plays a key role for the developmental switch in vascular inhibitory properties of the notochord. Evidence is also provided that the developmental loss of inhibitors coupled with persisting positive vascular factors promotes aortae fusion along the midline. This developmental switch of notochord activity explains how aortae fusion is signaled in amniote embryos.

MATERIALS AND METHODS
Immunostaining and whole-mount in situ hybridization
Japanese quail (*Cortunix japonica*) and chicken embryos (Red Rock) were staged by somite number according to Hamburger and Hamilton (Hamburger and Hamilton, 1951). Qh1 immunodetection was performed in whole-mount (Reese et al., 2004) and in frozen sections (Ishii et al., 2007) as previously described. Whole-mount in situ hybridization of chicken embryos was performed using similar methods to Hurtado and Mikawa (Hurtado and Mikawa, 2006), with antisense probes using digoxigenin- or fluorescein-labeled UTP (Roche) for synthesis of RNA probes from linearized DNA templates (Megascript, Ambion). Stained embryos were post-fixed in 4% paraformaldehyde in PBS and 10 μm paraffin wax sectioned by standard procedures. Approximate size references were based on an E2 embryonic condensed somite width of 70 μm.

Analysis of dorsal aortae width and notochord staining of Chordin and SHH
Chordin, *Shh* and *Cx40* transcripts were visualized by in situ hybridization with substrates for alkaline phosphate, NBT/BCIP (dark purple; 3 μl of 100 mg/ml NBT and 3 μl of 50 mg/ml BCIP) and BCIP alone (light blue; 15 μl of 50 mg/ml BCIP). Images were captured and processed using Adobe Photoshop software. ImageJ (v1.37) gel analyzer software was used to determine staining intensity of non-saturated whole-mount in situ hybridization BCIP-stained notochord regions at 150 μm intervals along the AP axis starting with the narrowest anterior region. The corresponding width of the avascular space was recorded and these values were plotted using Microsoft Excel.

Real-time PCR
Isolated notochord regions or embryos were homogenized with Trizol (Invitrogen) and total RNA was extracted using the manufacturer's protocol. Total RNA was DNase (New England Biolabs) treated and converted to cDNA by oligo DT priming using SuperScript II First-Strand Synthesis (Invitrogen). Real-time PCR was carried out using iQ SYBR Green (Bio Rad) on an iQ5 iCycler (Bio Rad) according to the manufacturer's protocol using the Livak method with ODC (C_T) values as a reference and β-actin as a supporting control. Primer pairs amplify 100-130 nucleotide regions designed to bridge separate exons where genomic evidence exists. Each real-time PCR result was performed in duplicate with standard deviation of C_T less than 0.3. Primer sequences and annealing temperatures are provided in Table S1 in the supplementary material.

Embryo culture
Quail eggs were incubated at 38°C in a humid environment until the desired stage. Embryos were removed from the egg and cultured on egg agar plates dorsal side down (Chapman et al., 2001). Under our modified New culture, quail embryos exhibited dorsal aortae fusion one stage earlier, on average, than similarly staged in ovo sibling embryos (see Table S4 in the supplementary material).

Notochord implantation
Notochords from stage 10 or stage 17 chicken embryos were isolated, rinsed with PBS, trimmed into 200 μm lengths, and implanted into stage 4-5 quail hosts lateral to the primitive streak, via incision through the endoderm at a posterior region of the primitive streak. The embryos were re-incubated until stages 10-11 and processed for Qh1 immunostaining. In notochord replacement experiments, chick notochords were removed from stage 16-17 donors, trimmed into 500 μm lengths and implanted into stage 10 quail hosts, via an incision through the endoderm under the notochord spanning three somites at the eighth somite position. The host notochord was removed and replaced with a stage 16-17 chick donor notochord. In mock experiments, the host notochord was prepared for removal but left in place. In parallel, the host quail notochord was left in place and the stage 16-17 chick notochord was implanted 'overtop' through the incision in the endoderm. COS cell-mediated misexpression was performed by transfected COS1 cells with 1 μg of either *Rfp* or chick *Bmp4+Rfp* using standard procedures with Lipofectamine 2000 (Invitrogen). Similarly staged chick or quail notochords exhibited identical results to donor tissue (data not shown). Cell aggregates containing around 50 cells were inserted ventral to the notochord through an incision in the endoderm at the eighth somite of a stage 10 quail embryo. All embryos were reincubated for 6 hours or to the desired stage. Drug treatments were performed on stage 10 embryos cultured with two drops of 100 μM cyclopamine (Calbiochem) or 1-10 μM Ki8751 (Calbiochem) in Opti-MEM media. Cyclopamine was prepared as previously described (Vokes et al., 2004). Ki8751 was dissolved in DMSO and tested for activity through repression of VEGF-induced ERK phosphorylation in HAEC cells (data not shown).

HAEC assembly assays
To test whether notochords directly act on endothelial cells, we performed well-documented chord-forming assays (Arnaoutova et al., 2009; Kubota et al., 1988) using passages 2-4 of human aortic endothelial cells (HAECs) from Lonza cultured in a 96-well plate with the BD BioCoat Matrigel Angiogenesis System (BD Biosystems). Under these conditions, HAECs will assemble to form non-lumenated chords. Stage 10 or 17 isolated chick notochords were inserted 0.5 mm under the surface of the matrigel prior to addition of HAECs and cultured overnight. Cells were visualized using calcein staining (Invitrogen).

Electroporation
Expression plasmid DNA encoding Rfp, Chordin, BMP4, VEGF-164 or SHH was electroporated into stage 5 embryos as previously described (Hardy et al., 2008). Briefly, three 25 msecond pulses of 5 V spaced 1 second apart were generated using a BTX ECM 830 Genetrode 1 mm gold-plated electrodes (model 516) (Harvard Apparatus, MA) with a space of 2 mm between electrodes. DNA was prepared using Nucleobond AX nucleic acid purification (Macherey-Nagel). DNA (500 pl of a 1 μg/μl solution) containing 0.01% Fast Green dye (Sigma-Aldrich) was microinjected over the node on the dorsal side of the embryo between the epiblast and vitelline membrane (Femtojet, Ependorf). Resulting embryos exhibited transgene expression in the neural tube, non-neural ectoderm and notochord, with much lower efficiency in the notochord. *Shh* levels were directly determined by RT-PCR, while *Vegf* levels were estimated using qPCR with human and chick *Vegf* primers with nearly identical amplification efficiencies exhibiting mean levels detected at 1.9 times (s.d.=0.54/*n*=6) and 3.2 times (s.d.=2.05/*n*=4) greater than endogenous transcript levels.

RESULTS
Anterior to posterior wave of dorsal aortae fusion under the notochord
Until stage 10 (Hamburger and Hamilton, 1992), the dorsal aortae are bilateral vessels that lie on either side of an avascular space ventral and lateral to the notochord occupying the full lateral border somite (Fig. 1A). The first sign of fusion was the narrowing of the
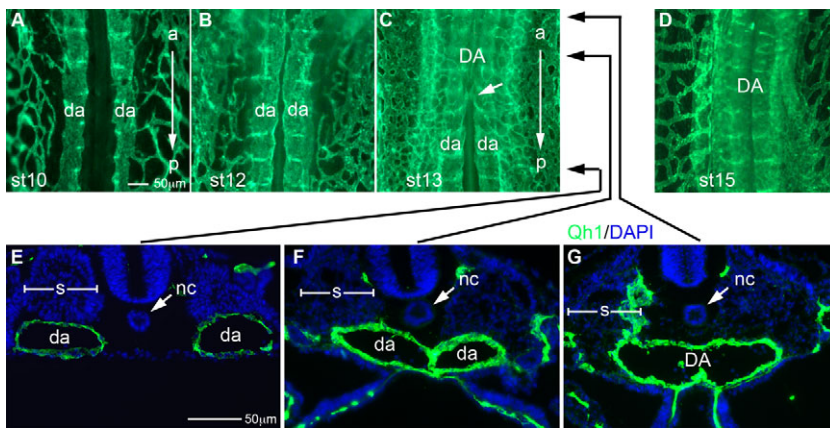
Fig. 1. The dorsal aortae fusion along the AP axis.
(**A-D**) Ventral views of quail embryos (somite level 6 to 13) stained with Qh1 (Green) for endothelial cells. (A) Stage 10 pre-fusion embryo. Dorsal aortae positioned lateral to the midline. (B) Stage 12 pre-fusion embryo showing narrowing of the midline avascular space. (C) Stage 13 fusion-stage embryo. Dorsal aortae fused at anterior regions (until white arrow) but remained unfused in posterior regions. (D) Stage 15 embryo with a fused DA. (**E-G**) Transverse sections of a stage 13 embryo double stained with Qh1 (green) and DAPI (blue). The dorsal aortae are unfused in a posterior region (E) and fused in anterior regions (F,G). Somites are indicated, showing medial positioning of fusing aortae. Scale bars: 50 µm. DA, dorsal aorta; da, dorsal aortae; nc, notochord; s, somite.

avascular space initiating at the anterior region of the embryo at stage 11. By stage 12 the avascular space substantially narrowed, particularly at anterior regions of the embryo (Fig. 1B). As development proceeded, the dorsal aortae were positioned medially relative to the somite, made direct contact with one another and fused under the notochord forming a single vessel while still remaining separated at posterior regions of the embryo (Fig. 1C,E-G). Fusion events occur concurrently with the turning of the embryo that presumably places the aortae, and somites, in closer proximity. Aortae fusion is propagated anteroposteriorly in later stages of development and the aortae zippered together along the midline (Fig. 1D) down to the level of the umbilical artery by the following day of development. The aortae fuse over much of the embryonic axis, with the exception of the posterior trunk and region anterior to the initial fusion site that remains bifurcated as the aortae connect to the heart outflows. The site of fusion was conserved among chicken and quail embryos of the same embryonic stage. Fusion first became detectable at stage 13. In subsequent stages examined (stages 14-15), the most posterior point of dorsal aortae fusion occurred at a specific somite position (somite 11 at stage 13; somite 14 at stage 14; somite 16 at stage 15) (see Table S2 in the supplementary material). Thus, the fusion of the dorsal aortae occurs from anterior to posterior, with the resulting DA forming under the notochord. Additionally, the latest position of dorsal aortae fusion was highly predictable at a given embryonic stage, suggesting that DA fusion is a tightly regulated process along the anteroposterior (AP) axis controlled in a stage-specific manner.

Developmental change in regulatory activities of the notochord

The pre-fusion-stage notochord creates a zone of vascular inhibition, thereby keeping the dorsal aortae apart (Reese et al., 2004; Bressan et al., 2009). However, these studies do not explain how the notochord allows the dorsal aortae to fuse along it later in development. We tested the possibility that regulatory properties of the notochord change during embryo development. Notochords from donor chick embryos isolated either from pre-fusion (stage 9-10) or fusion (stage 16-17) stages were implanted into a region lateral to the midline of host quail embryos at stages 4-5 (prior to formation of blood vessels). We then examined the resulting blood vessel development. The implanted pre-fusion notochords inhibited local blood vessel development at the implanted site, particularly overlying the endoderm of the embryo (Fig. 2A-C), consistent with our previous studies. By striking contrast, notochords derived from fusion-stage donors did not show clear inhibition of local blood

vessel formation (Fig. 2D-F). Despite the presence of implanted notochord, vessels formed over the endoderm. Furthermore, endothelial cells were detected in direct contact with the implanted notochord (Fig. 2F). This result shows that regulatory activities of notochords change as embryos develop, and that, at the stages following dorsal aortae fusion, notochords do not exert an inhibitory influence on vessel development in vivo.

To examine whether the above loss in vessel-suppressing activity by fusion-stage notochords was mediated directly on endothelial cells or indirectly through surrounding embryonic tissues, we analyzed effects of notochords at various developmental stages on cell assembly of human aortic endothelial cells (HAECs). In the absence of a notochord, HAECs assembled into endothelial cell chords that formed complex networks in culture, as well documented previously (Arnaoutova et al., 2009; Kubota et al., 1988). When a pre-fusion-stage notochord was placed in the matrix, the HAECs did not assemble around the co-cultured notochord fragment (Fig. 2H). Instead, HAECs assembled in regions where no notochord fragments were present, suggesting that pre-fusion-stage notochords act directly on endothelial cells and signal to inhibit their assembly (Fig. 2A-C). By contrast, fusion-stage notochords showed reduced inhibition of HAEC assembly, and HAECs assembled over the notochord (Fig. 2I). These results suggest that at the time of dorsal aortae fusion the notochord has no detectable inhibitory influence on endothelial cells.

Chordin levels decrease in the notochord as the dorsal aortae fuse

To determine the molecular signals that underlie the switch in inhibitory properties of the notochord, we examined the expression of vascular regulators in the notochord using real-time PCR. Analyzed genes were all secreted positive and negative vascular factors expressed in the notochord during dorsal aortae fusion. Putative 'negative factors' have activities to inhibit growth, migration and differentiation of endothelial cells, while 'positive factors' promote these activities. Our list of known negative factors expressed by the embryonic notochord during fusion stages included BMP antagonists chordin (*Chrd*) and noggin (*Nog*), activin inhibitors follistatin (*Fst*) and follistatin-like 1 (*Fstl1*), and the semaphorin 3 homologs (*Sema3a*, *Sema3d*, *Sema3e* and *Sema3f*). Of the negative factors, we identified *Chrd* as the most widely expressed in the notochord and most substantially decreased in expression in the notochord just prior to and during dorsal aortae fusion (see Fig. 3A and see Fig. S1 in the supplementary material). For example, in a stage 14 embryo there was a 93% decrease in *Chrd* levels in the
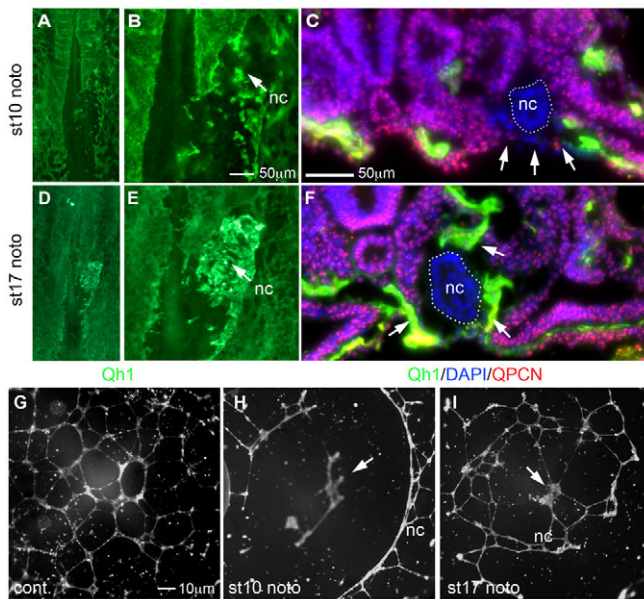
Fig. 2. Pre-fusion- and fusion-stage notochords differentially regulate endothelial cell assembly. (**A**) Quail embryo with stage 10 pre-fusion chick notochord implantation (nc) stained with Qh1 (green). (**B**) Higher magnification of A. Pre-fusion notochord inhibited local blood vessel assembly (eight out of nine embryos). (**C**) Section through the implantation site. Endothelial cells (arrows) are absent on the ventral surface of the embryo under the implanted stage 10 chick notochord (nc, white dots) within the surrounding quail host tissue marked with QPCN (red). (**D**) As in A but implanted fusion-stage chick notochord (stage 17). (**E**) Higher magnification of D. Endothelial cells accumulate in high numbers at the implanted site (12 out of 13 embryos). (**F**) As in C but with implantation of fusion-stage notochord showing endothelial cells directly surrounding the implanted stage 17 chick notochord (arrows). (**G**) Control human aortic endothelial cells (HAECs) assembled into chords. (**H**) HAECs assembled at a distance from a co-cultured pre-fusion chick notochord (stage 10) in all experiments (*n*=9). (**I**) HAECs assembled directly over a fusion-stage notochord (stage 17) in all but one experiment (*n*=12). nc, notochord.

Fig. 3. **Vascular factors in notochords.** Levels of negative (**A**) and positive (**B**) factors in pre-fusion notochords (stage 10 and posterior region of stage 14) and fusion-stage notochords (anterior region of stage 14 and stage 17). The abundance of Chrd is based on cycle number: there is a substantial drop in *Chrd* levels in fusion-stage notochords (asterisks) but nearly identical positive factor levels in pre-fusion and fusion regions of stage 14 notochords.

notochord over a fused DA compared with the adjacent posterior notochord region over an unfused region. Whole-mount in situ hybridization analysis showed that *Chrd* expression occurred throughout the notochord at pre-fusion stages (Fig. 4A), then decreased in the anterior region of the notochord while remaining high in posterior regions of the notochord during fusion stages (Fig. 4B,C). The downregulation of *Chrd* in the notochord along the AP axis progressed posteriorly in successive stages of embryonic development with *Chrd* expression becoming limited to the most posterior regions of the notochord by stage 15 (Fig. 4C). Other BMP antagonists, such as Noggin, were detected at much lower levels in the notochord compared with Chrd (Fig. 3A) consistent with previous publications (Connolly et al., 1997; Nimmagadda et al., 2005). Alternatively, our expression data showed that *Bmp4*, *Shh* and *Vegf* were detected equally well along the AP axis of fusion-stage embryos, despite the fact that these stages in development exhibited uneven fusion along the AP axis (Fig. 3B; Fig. 4D-I). Similarly, broad distribution of BMP2, BMP5 and BMP7 ligands was also apparent in fusion-stage embryos. BMP receptors showed nearly ubiquitous expression along the anteroposterior axis, including in the endothelial cells of the aortae (see Fig. S2 in the supplementary material) as previously reported (Andree et al., 1998; Hyer et al.,
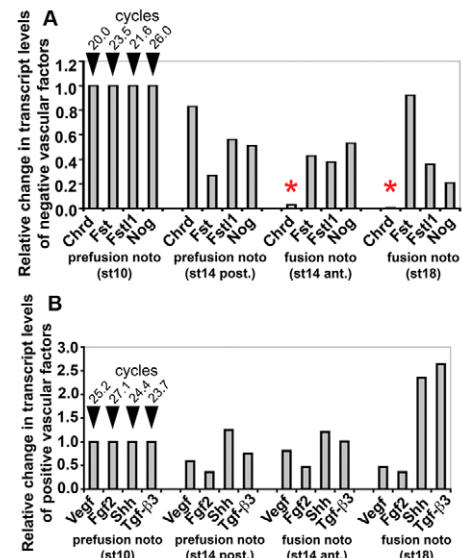
2003; McPherson et al., 2000; Reese et al., 2004; Streit et al., 1998). These data demonstrate that *Chrd* levels decrease in the notochord during dorsal aortae fusion, while positive factors, expressed in the notochord or broadly in the embryo, remain largely unchanged. The expression data further support a model in which dorsal aortae fusion occurs due to a loss of negative factors in the notochord in the presence of sustained levels of positive factors.

Downregulation of Chrd precedes dorsal aortae fusion

If the anteroposterior wave of *Chrd* downregulation in the notochord is a cause of dorsal aortae fusion, *Chrd* downregulation must occur prior to or at aortae fusion. To test this possibility, we performed double whole-mount in situ hybridization analysis in pre-fusion- (stage 12) (Fig. 4J,K) and fusion-stage embryos (stage 13-14) (Fig. 4L,M). Downregulation of *Chrd* in the notochord closely preceded narrowing of the avascular space and subsequent aortae fusion (Fig. 4K-M). To quantify this relationship, comparative analysis of *Chrd* staining intensity in the notochord with the width of the avascular space at the corresponding location along the AP axis showed a linear correlation (Fig. 4K,N). By contrast, *Shh* expression in the notochord and aortae fusion showed no clear relationship (Fig. 4J,N). The data show that as *Chrd* levels decreased in the notochord, the width of the avascular space also decreased. Transverse sections of double-hybridized embryos further revealed that the aortae remain far apart when *Chrd* is expressed in the notochord (Fig. 4O,P), and as levels of *Chrd* become undetectable, the avascular space shrinks and the aortae fuse (Fig. 4Q,R). Additional comparisons of *Chrd* downregulation and aortae fusion showed that between stage 13 and stage 15 the site of fusion occurs four or five somite positions after *Chrd* levels were undetectable in the notochord by whole-mount in situ hybridization (Fig. 4L,M; see Table S3 in the supplementary
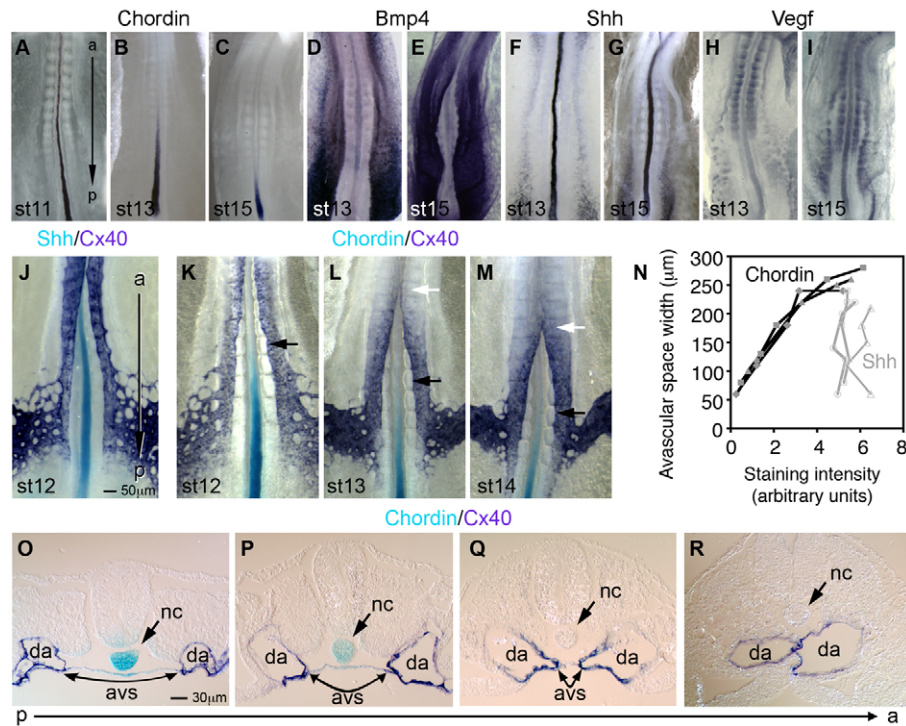
Fig. 4. Whole-mount in situ hybridization analysis for negative and positive embryonic vascular factors in pre-fusion and fusion-stage notochords. (**A-I**) Ventral views of chicken embryos stained for *Chrd*, *Bmp*4, *Shh* and *Vegf*, respectively. *Chrd* was expressed throughout the notochord of a stage 11 embryo (A), became downregulated along the AP axis as the embryo developed (B), and was expressed only in the posteriormost region of the notochord at stage 15 (C). By contrast, *Bmp*4 was expressed broadly lateral to the midline at both stages 13 (D) and 15 (E). No developmental change was evident for either *Shh* (F,G) or *Vegf* (H,I) between stages 13 and 15. (**J**) Double in situ hybridization for *Shh* and *Cx40* at stage 12. (**K-M**) Double in situ hybridization for *Chrd* and *Cx40,* at stages 12, 13 and 14, respectively. The latest position of the dorsal aortae fusion (white arrows) was detected consistently at five somite levels anterior to *Chrd* detection (black arrow). (**N**) Correlation assays between avascular space and the staining intensity of *Chrd* and *Shh* along the AP axis of stage 12 chick embryos (see Materials and methods section for further description). (**O-R**) Transverse sections of a stage 13 embryo double in situ hybridization for *Chrd* and *Cx40*. There is a wide avascular space where the notochord still highly expressed *Chrd*, whereas dorsal aortae are fused where notochord downregulated *Chrd*. avs, avascular space; da, dorsal aortae; nc, notochord.

material). The data clearly demonstrate that dorsal aortae fusion positively correlates with an AP wave of downregulation of *Chrd* in the notochord.

Maintenance of Chrd in the notochord is sufficient to inhibit dorsal aortae fusion

To test whether maintaining *Chrd* expression blocked fusion, we misexpressed Chrd at the midline. Through electroporation we co-expressed *Chrd* and red fluorescent protein (*Rfp*) along the midline of dorsoaxial embryonic tissues (Fig. 5). Misexpression of control *Rfp* alone allowed the dorsal aortae to fuse (Fig. 5A,B). By contrast, co-expression of *Chrd* and *Rfp* inhibited dorsal aortae fusion with the aortae remaining under the somite despite the turning of the embryo (Fig. 5C,D). The data indicate that continued expression of *Chrd* in areas where *Chrd* is normally downregulated (see Fig. 4B) is sufficient to inhibit dorsal aortae fusion and maintain the bilaterality of the dorsal aortae at least until stage 13. *Nog* misexpression not only inhibited fusion of the aortae but also disrupted capillary plexus formation at the adjacent area and expanded the lateral border of the somite (see Fig. S3 in the supplementary material), consistent with the described activity of Nog and Chrd (Streit and Stern, 1999; Tonegawa et al., 1997; Tonegawa and Takahashi, 1998). Our midline electroporation protocol proved useful for misexpressing transgenes along the AP axis, which altered the composition of signals for molecular interactions between the notochord and dorsal aortae.

The above results further support the idea that *Chrd* downregulation is crucial for signaling dorsal aortae fusion. To further test this model, we interfered with Chrd function by misexpressing *Bmp4*, as no method is currently available to lower *Chrd* levels in a notochord-specific manner in the avian system. Embryos with misexpressed *Bmp4*, by midline electroporation (Fig. 5G,H; see Fig. S4 in the supplementary material) or cell aggregates (Fig. 5K,M,O), exhibited precociously and ectopically fused vessels at the midline compared with stage 11 controls, which showed no midline vessels (Fig. 5E,F,I,N). *Bmp4* electroporations also resulted in malformations of axial tissues, including defective neural tube closure and somite condensation (Fig. 5; see Fig. S4 in the supplementary material). BMP4-expressing cell aggregates allowed for more precise temporal control of BMP misexpression. Indeed, this approach was sufficient to induce local sites of endothelial cell fusion, or endothelial cell bridges between the aortae without the widespread axial defects observed in electroporated embryos. Although induced sites of fusion may not exactly replicate the bona fide aortae fusion, blood flow between bilateral dorsal aortae through these connections was evident, indicating that BMP4-induced local fusions or endothelial cell bridges were a functional lumenated vessel system (Fig. 5P-T; see Movie S1 in the supplementary material). The induced vascular phenotype was consistent with the idea of BMP-dependent suppression of *Chrd* function along the midline.
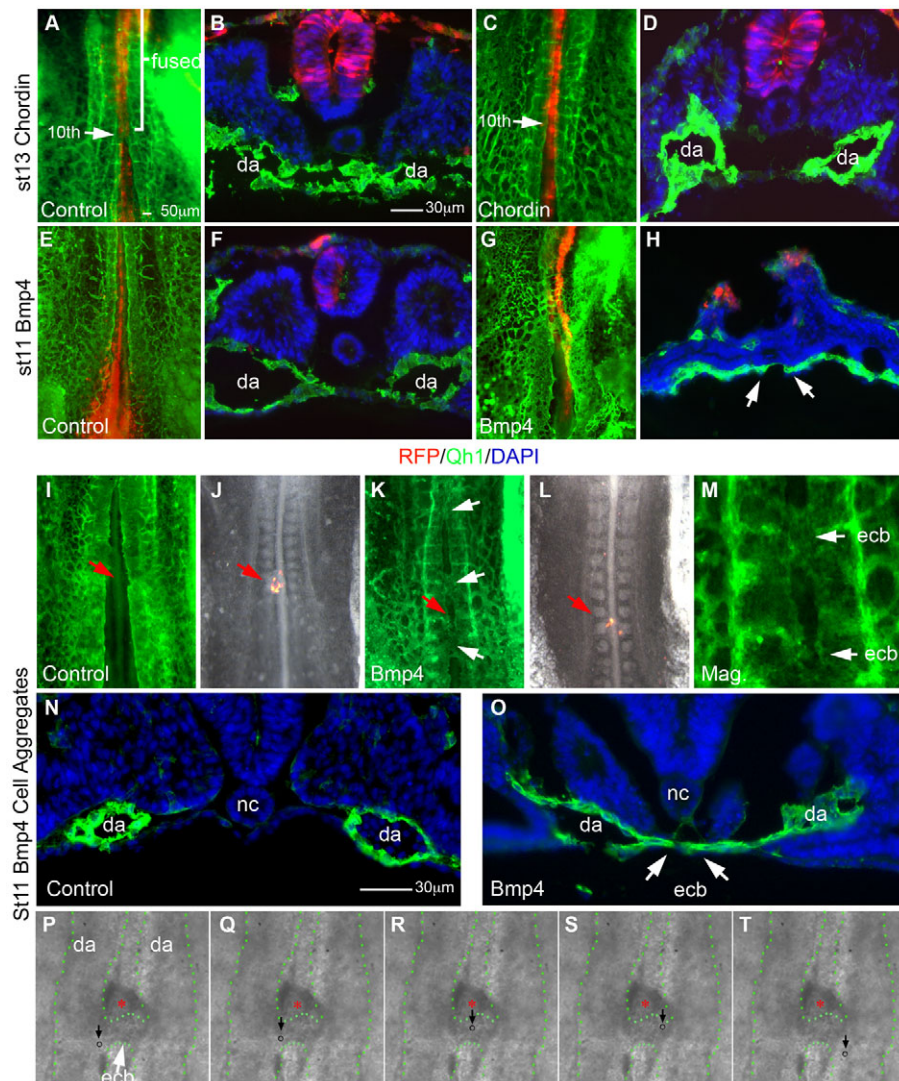
Fig. 5. Misexpression of Chrd and BMP4 is sufficient to regulate dorsal aortae fusion. Whole-mount and sectioned embryos imaged for direct RFP fluorescence (red), endothelial-specific Qh1 antibody (green) and DAPI nuclear counterstain (blue) in sections. (**A**) *Rfp*-electroporated control embryo at fusion stage (stage 13) showing fused dorsal aortae at the 10th somite position (*n*=11). (**B**) Transverse section of A, showing normally fused dorsal aortae below RFP-expressing tissues. (**C**) *Chrd+Rfp* electroporated embryo showing successful inhibition of dorsal aortae fusion in 84% of embryos (*n*=13). (**D**) Section of C showing that bilateral dorsal aortae remained unfused. (**E,F**) As in A,B but pre-fusion-stage control embryo (stage 11) showing unfused bilateral dorsal aortae (*n*=11). (**G,H**) As in E,F but *Bmp4+Rfp* electroporated embryo showing midline vessels and fused aortae-like vessels (arrows). Midline vessels occurred in all BMP4-expressing embryos (*n*=20). (**I**) Pre-fusion stage 11 control embryo with implanted RFP-expressing cell aggregates (red arrow) showing bilateral dorsal aortae (*n*=11). (**J**) As in I but a composite of RFP and bright-field images visualizing RFP-expressing cell aggregates (arrow). (**K**) As in I but BMP4-expressing cell aggregates (red arrow) exhibit several fused regions of the dorsal aortae (white arrows, occurring in nine out of 17 embryo). (**L**) Composite of RFP and bright-field images of K. Note the BMP4+RFP expressing cell aggregates between two fused regions of the dorsal aortae. (**M**) Magnified view of fused regions (white arrows) of the dorsal aortae in L,K. (**N**) Transverse section of control pre-fusion-stage embryo with bilateral dorsal aortae near the cell aggregates (not in view). (**O**) As in N but with BMP-expressing cell aggregate implantation (not in view). (**P-T**) Sequence of still images from Movie S1 in the supplementary material showing path of single blood cells (circles/arrows) moving through an endothelial cell bridge between the aortae induced by BMP4-misexpression (red asterisks). Dorsal aortae and endothelial cell bridge are outlined by green dots. ecb, endothelial cell bridge; da, dorsal aortae; nc, notochord.

The vessel promoting factors SHH and VEGF are necessary but not sufficient for aortae fusion

Although the above data show that suppression of notochord inhibitory activities by BMP at the midline is sufficient to signal dorsal aortae fusion, it is unclear whether BMP, which is expressed broadly throughout the embryo, is sufficient to guide the DA to fuse at the midline. We hypothesized that another positive input from the midline may play a role in positioning the dorsal aortae. Consistent with this model, suppression of either midline-expressed

positive vascular factor, SHH or VEGF, inhibited aortae fusion (Fig. 6; see Fig. S5 in the supplementary material). Double whole-mount in situ hybridization for *Chrd* and a dorsal aortae marker *Connexin40* (*Cx40*) revealed that the aortae fusion seen in control embryos (Fig. 6A,B) was dramatically suppressed in those treated with inhibitors to SHH (Fig. 6C,D) and VEGF (Fig. 6E,F). The results are consistent with known function of these factors in vascular patterning (Drake and Little, 1995; Kolesova et al., 2008; Nagase et al., 2006; Poole et al., 2001; Vokes et al., 2004). The data
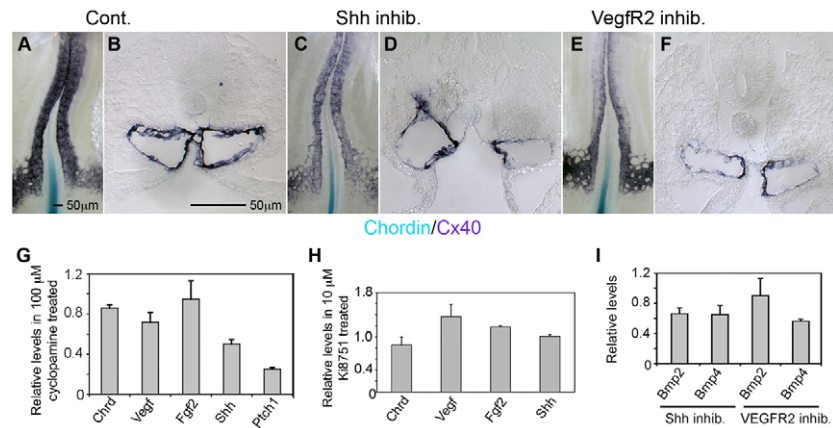
Fig. 6. The midline-positive signals SHH and VEGF are necessary for dorsal aortae fusion independent of Chrd. (**A**) Whole-mount double in situ hybridization for *Chrd* (blue) and *Cx40* (purple) in control embryo showing fused dorsal aortae at several somite levels anterior to *Chrd* downregulation in the notochord (*n*=10). (**B**) Transverse section of A showing fusing dorsal aortae under a Chrd(–) notochord. (**C**) As in A but treated with 100 μM cyclopamine (a hedgehog inhibitor) from stage 10 to stage 13, showing unfused dorsal aortae even though *Chrd* was downregulated in the notochord [as seen in control (*n*=9)]. (**D**) Transverse section of C. (**E**) As in C but treated with 10 μM Ki8751 (a VEGFR2 inhibitor) showing unfused dorsal aortae despite *Chrd* downregulation (*n*=8). (**F**) Section of E. (**G,H**) RT-PCR analysis of levels of *Chrd*, *Vegf*, *Fgf2*, *Shh* and *Ptch1* in embryos treated with cyclopamine and Ki8751, respectively. (**I**) RT-PCR for *Bmp2* and *Bmp4* in cyclopamine- and Ki8751-treated embryos. Error bars indicate s.d. of two replicate experiments containing three pooled sibling embryos.

also demonstrate that the function of midline positive vascular signals is necessary for dorsal aortae fusion when *Chrd* is already downregulated in the notochord.

To test possible crosstalk between BMP, VEGF and hedgehog signaling under our experimental condition, vascular factor expression in embryos with inhibitor treatments was examined using real-time PCR. Cyclopamine treatments, to inhibit Hedgehog signaling, showed expected decreases in *Shh* and the receptor *Ptch1*, which are known targets of hedgehog signaling (Marigo and Tabin, 1996; Sanz-Ezquerro and Tickle, 2000) (Fig. 6G). No substantial changes in *Chrd*, *Fgf2*, *Vegf*, *Bmp2* or *Bmp4* levels were observed after cyclopamine treatments. In embryos with inhibited VEGF signaling, no change in *Chrd* levels was detected, though small increases in *Vegf*, *Fgf2*, *Shh* and *Bmp2*, and a decrease in *Bmp4* levels were detected. The data show that midline vascular factors SHH and VEGF are required for aortae fusion, although inhibiting SHH or VEGF has additional influence on other growth factor signaling pathways relevant to vascular patterning. Therefore, we tested whether elevating the levels of these factors was sufficient to induce aortae fusion. Using our electroporation method, *Shh* or *Vegf* as misexpressed at the embryonic midline at stage 5-6, cultured to stage 11 and assayed for ectopic or early aortae fusion (Fig. 7). When misexpressed, neither *Shh* nor *Vegf* induced precocious fusion. Although *Shh* and *Vegf* misexpression resulted in substantial increases in these factors at the midline compared with total embryonic expression (75% and 183% increase respectively, detected by real time PCR), no ectopic or early aortae fusion occurred. Taken together, the data show that the continued presence of *Shh* and *Vegf* is necessary, but not sufficient to signal dorsal aortae fusion.

Notochords lacking Chrd expression signal dorsal aortae fusion

The above data suggest that as long as positive factors are present, suppression of BMP antagonist action alone is sufficient to signal fusion. To test this directly, we replaced a region of notochord known to express high levels of *Chrd*, Chrd(+), with one expressing low

levels of *Chrd*, Chrd(–). A section of notochord in a stage 9-10 host quail embryo where expression of Chrd was evident (Fig. 4A) was replaced with an anterior segment of a stage 17 donor chick
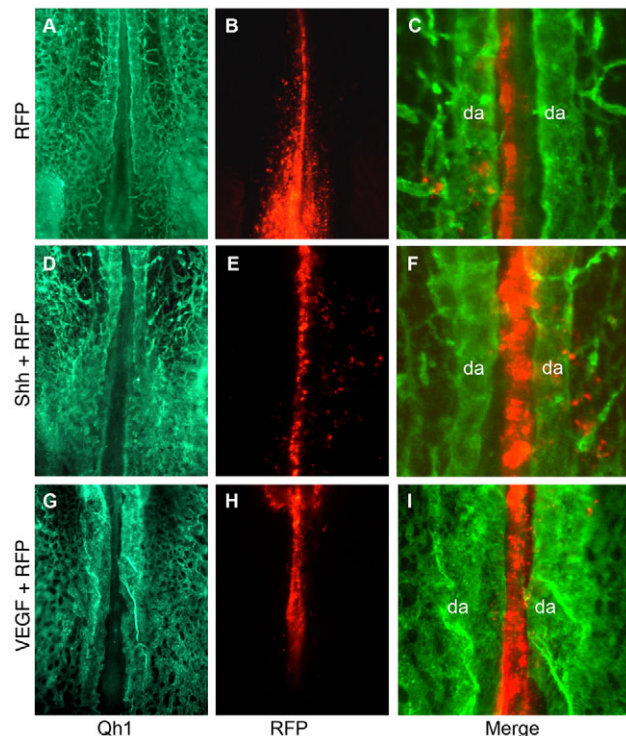

Fig. 7. The midline-positive signals SHH and VEGF are not sufficient to signal dorsal aortae fusion. (A-I) Stage 11 electroporated embryos imaged for vascular-specific Qh1 antibody (A,D,G), direct RFP fluorescence (B,E,H) and magnified overlay of Qh1 and RFP (C,F,I). (**A-C**) Control RFP embryo with unfused dorsal aortae (*n*=11). (**D-F**) *Shh+Rfp* electroporated embryo showing no midline vessels or dorsal aortae fusion (*n*=8). (**G-I**) *Vegf+Rfp* electroporated embryo showing enlarged dorsal aortae but no dorsal aortae fusion (*n*=9). da, dorsal

notochord where little or no expression of Chrd was detectable (Fig. 3A, Fig. 4C). In mock experiments, the host exhibited no midline vessels at the site of dissection (Fig. 8A,B). By contrast, implantation of a Chrd(−) notochord resulted in midline spanning vessels (Fig. 8C,D). The data demonstrate that a notochord from a fusion-stage embryo, no longer expressing *Chrd*, is sufficient to signal fusion in a pre-fusion-stage embryo. To discern increased positive signaling from decreased negative signaling, a Chrd(−) chick notochord was implanted without removing the endogenous Chrd(+) notochord of host quail embryos (Fig. 8E,F). The resulting embryos exhibited no fusion where the Chrd(−) notochord was implanted and resembled mock experiments (Fig. 8B). The data demonstrate that a notochord expressing little or no Chrd is sufficient to signal fusion. This result is consistent with the model in which dorsal aortae fusion is mediated by a developmental decrease in inhibitory signaling rather than increased positive signaling.

DISCUSSION

The present study identified a novel mechanism of vascular remodeling where vessel fusion occurs via a downregulation of negative vascular factors in the continued presence of positive vascular factors. The tissue that signals aortae fusion is the notochord. Prior to fusion the notochord expresses both positive and negative factors that, when combined, exert a net negative influence and block the initiation of aortae fusion. It is through the downregulation of negative vascular factors in the presence of sustained levels of positive vascular factors that the inhibitory influence of the notochord is lost and aortae fusion is signaled. What follows is a remarkable rearrangement of cell and tissue architecture to merge two vessels into one without disrupting vessel integrity. Although the complexity of cellular interactions to physically fuse two vessels is probably astonishing, the mechanism to signal the fusion is the downregulation of a few negative vascular factors by the notochord.

How do the aortae fuse? Although the paired aortae are separated by a substantial distance across the midline, they must be repositioned to the midline to be in proximity to fuse. It would be plausible that this process may be, in part, achieved as a passive consequence of the lateral body folding of the embryo, which repositions the somite and associated aortae to be closer together. Although this physical mechanism cannot be ruled out, our data show that initiation of fusion via narrowing of the avascular zone and initial bridging of the aortae occur prior to embryonic turning and this process is regulated by paracrine signaling. This medial movement of the aortae is also referred to as a narrowing of the avascular space with the aortae being repositioned from directly under the somite to under the notochord. Our data support the idea that this movement and the eventual lateral contact of the aortae require positive vascular signals and are inhibited by notochord expression of BMP antagonist. It is also unclear what role endothelial cell adhesion between the aortae plays in the mechanics of fusion by 'zippering up' the aortae as cadherin 5 mutant mice show defective aortae fusion (Gory-Faure et al., 1999). Although our data show that paracrine signaling brings the aortae together, the mechanism of physically integrating the two aortae into a single vessel remains unclear. It is not known how adhesion and attachment of endothelial cells of the paired aortae is achieved. It remains unstudied whether the wall separating the aortae lumen is lost through apoptosis or if the lumenal wall cells are redistributed or to what extent regulation of cell polarity plays in this process as recently shown for the initial lumenization of the aortae (Strilic et al., 2009; Zovein et al., 2010).
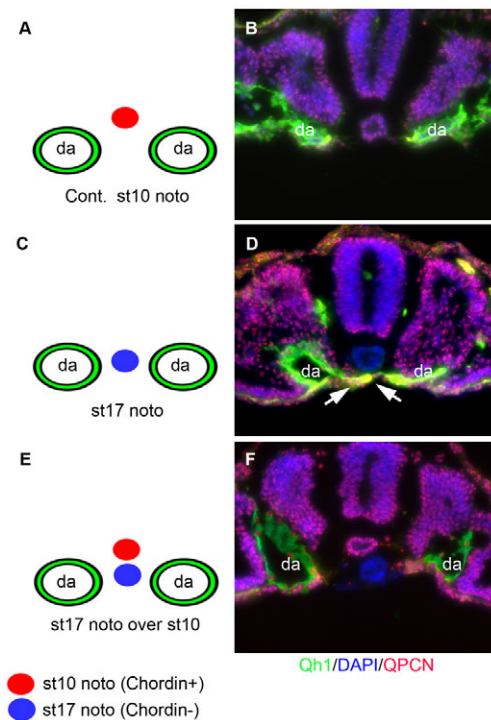
Fig. 8. Fusion-stage notochords can signal midline-spanning vessels. (**A**,**B**) Diagram and transverse section, respectively, of control mock dissection at a stage 10, cultured for 6 hours until stage 11 and triple stained for endothelial marker Qh1 (green), DAPI (blue) and quail-specific antigen QPCN (red). Bilateral dorsal aortae are normal (*n*=9). (**C**,**D**) As in A,B but the host stage 10 notochord has been replaced with a stage 17 notochord. Host dorsal aortae are fused in the prefusion-stage embryo under the implanted fusion-stage donor notochord (blue) (*n*=8). (**E**,**F**) As in A,B but implantation of a stage 17 chick notochord ventral to a stage 10 host quail notochord. Resulting embryo exhibiting bilateral dorsal aortae and no fusion (*n*=7). da, dorsal aortae.

Our data point to Chrd as the switch that regulates dorsal aortae fusion. Although other BMP antagonists show expression at the midline during earlier stages of development, prior to aortae fusion, Chrd is vastly more abundant than other BMP antagonists in the notochord and, thus, is an influential regulator of BMP signaling at the midline. When Chrd is expressed at the midline, aortae fusion does not occur. Aortae fusion is signaled when BMP signaling is restored by *Chrd* downregulation. The remarkable downregulation of *Chrd* along the AP axis closely precedes aortae fusion, implying a role in this process. It is unclear whether other BMP-dependent axial patterning events also use this signal (Dale et al., 1999; McMahon et al., 1998; Reshef et al., 1998; Tonegawa and Takahashi, 1998). How *Chrd* is regulated along the AP axis remains unknown. Survey of the GEISHA chicken EST database (http://geisha.arizona.edu/geisha/) does not identify other genes that share similar anteroposterior regulation. In addition, described regulators of *Chrd* from amphibian studies, such as *Lim1*, show no AP regulation in the notochord and become downregulated prior to dorsal aortae formation (GEISHA database) (Collart et al., 2005). Although Chrd appears to serve as the switch for aortae fusion, it remains unclear how the switch is regulated.

It is unexpected that BMP signaling plays such a pivotal role in aortae fusion as the strongest sources of BMP occur broadly throughout the embryo (Reese et al., 2004; Schultheiss et al., 1997;

Tonegawa et al., 1997). We reconcile this by proposing that a second positive vascular input, probably a non-BMP signal, secreted from the notochord, provides the midline-positioning signal. According to this model, BMP functions permissively, allowing for proper reception of other vessel-forming signals. How BMP performs this function is yet unclear; however, recently it has been shown that BMP positively regulates the receptors of vessel promoting factors including the VEGF receptor VEGFR2/FLK1 (Nimmagadda et al., 2007; Suzuki et al., 2008). Through this mechanism BMP modifies the ability of endothelial cells to respond to vessel forming signals; thus, in the absence of BMP signaling, endothelial cells are blind to VEGF. This could explain why endothelial cells do not arise from or migrate to where Nog and Chrd are expressed, despite the presence of VEGF, FGF2 or SHH (Bressan et al., 2009; Kang et al., 2009; Nimmagadda et al., 2005; Reese et al., 2004). It remains unclear whether BMP signals dorsal aortae fusion by regulating the expression of receptors of positive vascular factors. Although our data show that BMP is the only 'positive' vessel-forming signal capable of accelerating fusion and initiating ectopic sites of fusion, curiously, at sites of BMP-induced ectopic fusion, a bridge between the paired aortae, rather than a single midline vessel, is created. Aortae fusion does not occur fully as the lateral edges of the aortae remain near the lateral somite border. It is unclear whether this is merely a transitional state in aortae fusion or whether additional signals reposition the lateral boundaries of the aortae towards the midline. Thus, we cannot say that BMP causes fusion but rather that BMP is sufficient to initiate fusion.

Our data point to a role for SHH and VEGF as midline vascular signals to promote midline DA formation. Although *Shh*, but not *Vegf*, shows specific midline-enriched expression during fusion events (Reese et al., 2004), both are necessary for dorsal aortae fusion in avian and rodent embryos (Carmeliet et al., 1996; Kolesova et al., 2008; Nagase et al., 2006) and either factor has the activity needed to assemble vessels (Connolly et al., 1989; Vokes et al., 2004). VEGF and SHH may have independent activity in aortae fusion but it remains possible that SHH acts in a linear pathway to regulate VEGF and other vessel-promoting factors, including *Bmp2* and *Bmp4* (Lawson et al., 2002; Pola et al., 2001). Although, SHH and VEGF have evolutionary conserved roles in midline aorta positioning, neither factor was sufficient to promote precocious vessel fusion when misexpressed. Similarly, both widespread and local exogenous VEGF application fuses most of the embryonic vasculature, but not the dorsal aortae (Drake and Little, 1995; Poole et al., 2001). Furthermore, embryonic or extra-embryonic insufficiency of VEGF inhibits aortae formation complicating interpretation of the role of VEGF in subsequent aortae fusion (Carmeliet et al., 1996; Damert et al., 2002). These results illustrate the difficulty in identifying the exact midline positive signal and, more importantly, demonstrate that positive signals alone are not always sufficient to direct blood vessel growth and remodeling events. Taken together, our studies suggest that some vascular remodeling events also require a dampening of inhibitory signals.

Our data provide a novel mechanism of vascular patterning. Our model of regulation of dorsal aortae fusion may provide insights into other vessel patterning or remodeling, and may also serve as the basis for future therapeutic approaches to repair vascular injury and/or inhibit tumor angiogenesis.

Acknowledgements

Competing interests statement

Supplementary material

References

Andree, B., Duprez, D., Vorbusch, B., Arnold, H. H. and Brand, T. (1998). BMP-2 induces ectopic expression of cardiac lineage markers and interferes with somite formation in chicken embryos. *Mech. Dev.* **70**, 119-131.

Arnaoutova, I., George, J., Kleinman, H. K. and Benton, G. (2009). The endothelial cell tube formation assay on basement membrane turns 20, state of the science and the art. *Angiogenesis* **12**, 267-274.

Auguste, P., Javerzat, S. and Bikfalvi, A. (2003). Regulation of vascular development by fibroblast growth factors. *Cell Tissue Res.* **314**, 157-166.

Bressan, M., Davis, P., Timmer, J., Herzlinger, D. and Mikawa, T. (2009). Notochord-derived BMP antagonists inhibit endothelial cell generation and network formation. *Dev. Biol.* **326**, 101-111.

Carmeliet, P. V., Ferreira, V., Breier, G., Pollefeyt, S., Kieckens, L., Gertsenstein, M., Fahrig, M., Vandenhoeck, A., Harpal, K., Eberhardt, C. et al. (1996). Abnormal blood vessel development and lethality in embryos lacking a single VEGF allele. *Nature* **380**, 435-439.

Chapman, S. C., Collignon, J., Schoenwolf, G. C. and Lumsden, A. (2001). Improved method for chick whole-embryo culture using a filter paper carrier. *Dev. Dyn.* **220**, 284-289.

Cleaver, O. and Krieg, P. A. (1998). VEGF mediates angioblast migration during development of the dorsal aorta in Xenopus. *Development* **125**, 3905-3914.

Cleaver, O., Seufert, D. W. and Krieg, P. A. (2000). Endoderm patterning by the notochord: development of the hypochord in Xenopus. *Development* **127**, 869-879.

Collart, C., Verschueren, K., Rana, A., Smith, J. C. and Huylebroeck, D. (2005). The novel Smad-interacting protein Smicl regulates Chordin expression in the Xenopus embryo. *Development* **132**, 4575-4586.

Connolly, D. J., Patel, K. and Cooke, J. (1997). Chick noggin is expressed in the organizer and neural plate during axial development, but offers no evidence of involvement in primary axis formation. *Int. J. Dev. Biol.* **41**, 389-396.

Connolly, D. T., Heuvelman, D. M., Nelson, R., Olander, J. V., Eppley, B. L., Delfino, J. J., Siegel, N. R., Leimgruber, R. M. and Feder, J. (1989). Tumor vascular permeability factor stimulates endothelial cell growth and angiogenesis. *J. Clin. Invest.* **84**, 1470-1478.

Cox, C. M., D'Agostino, S. L., Miller, M. K., Heimark, R. L. and Krieg, P. A. (2006). Apelin, the ligand for the endothelial G-protein-coupled receptor, APJ, is a potent angiogenic factor required for normal vascular development of the frog embryo. *Dev. Biol.* **296**, 177-189.

Dale, K., Sattar, N., Heemskerk, J., Clarke, J. D., Placzek, M. and Dodd, J. (1999). Differential patterning of ventral midline cells by axial mesoderm is regulated by BMP7 and chordin. *Development* **126**, 397-408.

Damert, A., Miquerol, L., Gertsenstein, M., Risau, W. and Nagy, A. (2002). Insufficient VEGFA activity in yolk sac endoderm compromises haematopoietic and endothelial differentiation. *Development* **129**, 1881-1892.

Davis, S., Aldrich, T. H., Jones, P. F., Acheson, A., Compton, D. L., Jain, V., Ryan, T. E., Bruno, J., Radziejewski, C., Maisonpierre, P. C. et al. (1996). Isolation of angiopoietin-1, a ligand for the TIE2 receptor, by secretion-trap expression cloning. *Cell* **87**, 1161-1169.

Drake, C. J. and Little, C. D. (1995). Exogenous vascular endothelial growth factor induces malformed and hyperfused vessels during embryonic neovascularization. *Proc. Natl. Acad. Sci. USA* **92**, 7657-7661.

Dyer, M. A., Farrington, S. M., Mohn, D., Munday, J. R. and Baron, M. H. (2001). Indian hedgehog activates hematopoiesis and vasculogenesis and can respecify prospective neurectodermal cell fate in the mouse embryo. *Development* **128**, 1717-1730.

Gaur, P., Bielenberg, D. R., Samuel, S., Bose, D., Zhou, Y., Gray, M. J., Dallas, N. A., Fan, F., Xia, L., Lu, J. et al. (2009). Role of class 3 semaphorins and their receptors in tumor growth and angiogenesis. *Clin. Cancer Res.* **15**, 6763-6770.

Gory-Faure, S., Prandini, M. H., Pointu, H., Roullot, V., Pignot-Paintrand, I., Vernet, M. and Huber, P. (1999). Role of vascular endothelial-cadherin in vascular morphogenesis. *Development* **126**, 2093-2102.

Gospodarowicz, D. (1976). Humoral control of cell proliferation: the role of fibroblast growth factor in regeneration, angiogenesis, wound healing, and neoplastic growth. *Prog. Clin. Biol. Res.* **9**, 1-19.

Goumans, M. J., Valdimarsdottir, G., Itoh, S., Rosendahl, A., Sideras, P. and ten Dijke, P. (2002). Balancing the activation state of the endothelium via two distinct TGF-beta type I receptors. *EMBO J.* **21**, 1743-1753.

Gu, C., Yoshida, Y., Livet, J., Reimert, D. V., Mann, F., Merte, J., Henderson, C. E., Jessell, T. M., Kolodkin, A. L. and Ginty, D. D. (2005). Semaphorin 3E and plexin-D1 control vascular pattern independently of neuropilins. *Science* **307**, 265-268.

Haigh, J. J. (2008). Role of VEGF in organogenesis. *Organogenesis* **4**, 247-256.

Hamburger, V. and Hamilton, H. L. (1992). A series of normal stages in the development of the chick embryo. *Dev. Dyn.* **195**, 231-272.

Hardy, K. M., Garriock, R. J., Yatskievych, T. A., D'Agostino, S. L., Antin, P. B. and Krieg, P. A. (2008). Non-canonical Wnt signaling through Wnt5a/b and a novel Wnt11 gene, Wnt11b, regulates cell migration during avian gastrulation. *Dev. Biol.* **320**, 391-401.

Heimark, R. L., Twardzik, D. R. and Schwartz, S. M. (1986). Inhibition of endothelial regeneration by type-beta transforming growth factor from platelets. *Science* **233**, 1078-1080.

Hiraki, Y., Inoue, H., Kondo, J., Kamizono, A., Yoshitake, Y., Shukunami, C. and Suzuki, F. (1996). A novel growth-promoting factor derived from fetal bovine cartilage, chondromodulin II. Purification and amino acid sequence. *J. Biol. Chem.* **271**, 22657-22662.

Hiraki, Y., Kono, T., Sato, M., Shukunami, C. and Kondo, J. (1997). Inhibition of DNA synthesis and tube morphogenesis of cultured vascular endothelial cells by chondromodulin-I. *FEBS Lett.* **415**, 321-324.

Hogan, K. A. and Bautch, V. L. (2004). Blood vessel patterning at the embryonic midline. *Curr. Top. Dev. Biol.* **62**, 55-85.

Hurtado, R. and Mikawa, T. (2006). Enhanced sensitivity and stability in two-color in situ hybridization by means of a novel chromagenic substrate combination. *Dev. Dyn.* **235**, 2811-2816.

Hyer, J., Kuhlman, J., Afif, E. and Mikawa, T. (2003). Optic cup morphogenesis requires pre-lens ectoderm but not lens differentiation. *Dev. Biol.* **259**, 351-363.

Ishii, Y., Langberg, J. D., Hurtado, R., Lee, S. and Mikawa, T. (2007). Induction of proepicardial marker gene expression by the liver bud. *Development* **134**, 3627-3637.

Kane, R., Godson, C. and O'Brien, C. (2008). Chordin-like 1, a bone morphogenetic protein-4 antagonist, is upregulated by hypoxia in human retinal pericytes and plays a role in regulating angiogenesis. *Mol. Vis.* **14**, 1138-1148.

Kang, H. W., Walvick, R. and Bogdanov, A., Jr (2009). In vitro and In vivo imaging of antivasculogenesis induced by Noggin protein expression in human venous endothelial cells. *FASEB J.* **23**, 4126-4134.

Kolesova, H., Roelink, H. and Grim, M. (2008). Sonic hedgehog is required for the assembly and remodeling of branchial arch blood vessels. *Dev. Dyn.* **237**, 1923-1934.

Kubota, Y., Kleinman, H. K., Martin, G. R. and Lawley, T. J. (1988). Role of laminin and basement membrane in the morphological differentiation of human endothelial cells into capillary-like structures. *J. Cell Biol.* **107**, 1589-1598.

Lawson, N. D., Vogel, A. M. and Weinstein, B. M. (2002). sonic hedgehog and vascular endothelial growth factor act upstream of the Notch pathway during arterial endothelial differentiation. *Dev. Cell* **3**, 127-136.

Maeshima, K., Maeshima, A., Hayashi, Y., Kishi, S. and Kojima, I. (2004). Crucial role of activin a in tubulogenesis of endothelial cells induced by vascular endothelial growth factor. *Endocrinology* **145**, 3739-3745.

Maisonpierre, P. C., Suri, C., Jones, P. F., Bartunkova, S., Wiegand, S. J., Radziejewski, C., Compton, D., McClain, J., Aldrich, T. H., Papadopoulos, N. et al. (1997). Angiopoietin-2, a natural antagonist for Tie2 that disrupts in vivo angiogenesis. *Science* **277**, 55-60.

Marigo, V. and Tabin, C. J. (1996). Regulation of patched by sonic hedgehog in the developing neural tube. *Proc. Natl. Acad. Sci. USA* **93**, 9346-9351.

McMahon, J. A., Takada, S., Zimmerman, L. B., Fan, C. M., Harland, R. M. and McMahon, A. P. (1998). Noggin-mediated antagonism of BMP signaling is required for growth and patterning of the neural tube and somite. *Genes Dev.* **12**, 1438-1452.

McPherson, C. E., Varley, J. E. and Maxwell, G. D. (2000). Expression and regulation of type I BMP receptors during early avian sympathetic ganglion development. *Dev. Biol.* **221**, 220-232.

Nagase, T., Nagase, M., Yoshimura, K., Machida, M. and Yamagishi, M. (2006). Defects in aortic fusion and craniofacial vasculature in the holoprosencephalic mouse embryo under inhibition of sonic hedgehog signaling. *J. Craniofac. Surg.* **17**, 736-744.

Nimmagadda, S., Geetha Loganathan, P., Huang, R., Scaal, M., Schmidt, C. and Christ, B. (2005). BMP4 and noggin control embryonic blood vessel formation by antagonistic regulation of VEGFR-2 (Quek1) expression. *Dev. Biol.* **280**, 100-110.

Nimmagadda, S., Geetha-Loganathan, P., Scaal, M., Christ, B. and Huang, R. (2007). FGFs, Wnts and BMPs mediate induction of VEGFR-2 (Quek-1) expression during avian somite development. *Dev. Biol.* **305**, 421-429.

Oh, S. P., Seki, T., Goss, K. A., Imamura, T., Yi, Y., Donahoe, P. K., Li, L., Miyazono, K., ten Dijke, P., Kim, S. et al. (2000). Activin receptor-like kinase 1 modulates transforming growth factor-beta 1 signaling in the regulation of angiogenesis. *Proc. Natl. Acad. Sci. USA* **97**, 2626-2631.

Pardanaud, L., Altmann, C., Kitos, P., Dieterlen-Lievre, F. and Buck, C. A. (1987). Vasculogenesis in the early quail blastodisc as studied with a monoclonal antibody recognizing endothelial cells. *Development* **100**, 339-349.

Pola, R., Ling, L. E., Silver, M., Corbley, M. J., Kearney, M., Blake Pepinsky, R., Shapiro, R., Taylor, F. R., Baker, D. P., Asahara, T. et al. (2001). The morphogen Sonic hedgehog is an indirect angiogenic agent upregulating two families of angiogenic growth factors. *Nat. Med.* **7**, 706-711.

Poole, T. J., Finkelstein, E. B. and Cox, C. M. (2001). The role of FGF and VEGF in angioblast induction and migration during vascular development. *Dev. Dyn.* **220**, 1-17.

Reese, D. E., Hall, C. E. and Mikawa, T. (2004). Negative regulation of midline vascular development by the notochord. *Dev. Cell* **6**, 699-708.

Reshef, R., Maroto, M. and Lassar, A. B. (1998). Regulation of dorsal somitic cell fates: BMPs and Noggin control the timing and pattern of myogenic regulator expression. *Genes Dev.* **12**, 290-303.

Sanz-Ezquerro, J. J. and Tickle, C. (2000). Autoregulation of Shh expression and Shh induction of cell death suggest a mechanism for modulating polarising activity during chick limb development. *Development* **127**, 4811-4823.

Schultheiss, T. M., Burch, J. B. and Lassar, A. B. (1997). A role for bone morphogenetic proteins in the induction of cardiac myogenesis. *Genes Dev.* **11**, 451-462.

Senger, D. R., Galli, S. J., Dvorak, A. M., Perruzzi, C. A., Harvey, V. S. and Dvorak, H. F. (1983). Tumor cells secrete a vascular permeability factor that promotes accumulation of ascites fluid. *Science* **219**, 983-985.

Serini, G., Valdembri, D., Zanivan, S., Morterra, G., Burkhardt, C., Caccavari, F., Zammataro, L., Primo, L., Tamagnone, L., Logan, M. et al. (2003). Class 3 semaphorins control vascular morphogenesis by inhibiting integrin function. *Nature* **424**, 391-397.

Streit, A. and Stern, C. D. (1999). Mesoderm patterning and somite formation during node regression: differential effects of chordin and noggin. *Mech. Dev.* **85**, 85-96.

Streit, A., Lee, K. J., Woo, I., Roberts, C., Jessell, T. M. and Stern, C. D. (1998). Chordin regulates primitive streak development and the stability of induced neural cells, but is not sufficient for neural induction in the chick embryo. *Development* **125**, 507-519.

Strilic, B., Kucera, T., Eglinger, J., Hughes, M. R., McNagny, K. M., Tsukita, S., Dejana, E., Ferrara, N. and Lammert, E. (2009). The molecular basis of vascular lumen formation in the developing mouse aorta. *Dev. Cell* **17**, 505-515.

Suri, C., Jones, P. F., Patan, S., Bartunkova, S., Maisonpierre, P. C., Davis, S., Sato, T. N. and Yancopoulos, G. D. (1996). Requisite role of angiopoietin-1, a ligand for the TIE2 receptor, during embryonic angiogenesis. *Cell* **87**, 1171-1180.

Suzuki, Y., Montagne, K., Nishihara, A., Watabe, T. and Miyazono, K. (2008). BMPs promote proliferation and migration of endothelial cells via stimulation of VEGF-A/VEGFR2 and angiopoietin-1/Tie2 signalling. *J. Biochem.* **143**, 199-206.

Tonegawa, A. and Takahashi, Y. (1998). Somitogenesis controlled by Noggin. *Dev. Biol.* **202**, 172-182.

Tonegawa, A., Funayama, N., Ueno, N. and Takahashi, Y. (1997). Mesodermal subdivision along the mediolateral axis in chicken controlled by different concentrations of BMP-4. *Development* **124**, 1975-1984.

Vokes, S. A., Yatskievych, T. A., Heimark, R. L., McMahon, J., McMahon, A. P., Antin, P. B. and Krieg, P. A. (2004). Hedgehog signaling is essential for endothelial tube formation during vasculogenesis. *Development* **131**, 4371-4380.

Weinstein, B. M. (1999). What guides early embryonic blood vessel formation? *Dev. Dyn.* **215**, 2-11.

Zovein, A. C., Luque, A., Turlo, K. A., Hofmann, J. J., Yee, K. M., Becker, M. S., Fassler, R., Mellman, I., Lane, T. F. and Iruela-Arispe, M. L. (2010). Beta1 integrin establishes endothelial cell polarity and arteriolar lumen formation via a Par3-dependent mechanism. *Dev. Cell* **18**, 39-51.

Table S1. Primers used for real time PCR

Gene	Forward primer	Reverse primer	T$_A$
ODC	5'-TATGTGATGTCAAGACCAGCATG-3'	5'-GATACTCAATTCCACTTTCACAG-3'	63°C
Chordin	5'-CTCATCAAATGTGCCATCTGCACC-3'	5'-TGCCAGCTCTCGTTGTTGAGGTA-3'	65°C
Fstl1	5'-CAACCTGGTCAAGACTTGACTGA-3'	5'-TTACATCTCCTTGGTGCTCATCT-3'	63°C
Fst	5'-CTTATCCGAGCGAGTGTGCCATG-3'	5'-CTGGTCTTCATCTTCCTCTTCTT-3'	63°C
Shh	5'-ACTGGGTCTACTACGAGTCCAAG-3'	5'-AGCTTGGTGCCTCCATGCTCCA-3'	60°C
Patched1	5'-GAGGAGCTCCATCATTATGAG-3'	5'-CTTGACTGATGCCTTGACTCT-3'	60°C
Vegf	5'-AAGCACTTGTTTGTACAAGATCC-3'	5'-TGTTCCCCCTTCTTTTCCGCT-3'	60°C
hVegf	5'-AGGAGGAGGGCAGAATCATCA-3'	5'-GGGTTGAAGATGTACTCGATC-3'	60°C
Fgf2	5'-AGCAGAAGAAAGAGGAGTAGTAT-3'	5'-GAAACATTCCTCTGTTGCACATT-3'	63°C
β-Actin	5'-CTGTCTGGATTGGAGGCTCTATC-3'	5'-CAGTCCGGTTTAGAAGCATTTGC-3'	60°C
Noggin	5'-CCTATACACGTGGAACGATCTCG-3'	5'-CAGGTTTGCAGACCATGCCTTCT-3'	63°C
TGFβ3	5'-GTCCATGAGCCTAAAGGCTACTT-3'	5'-AACATAGTACAAGATCGTCAGTG-3'	63°C
Bmp2	5'-CAAGAGGCACGTTAGGATTAGC-3'	5'-GCTTGACGCTTTTCTCTTTTGT-3'	60°C
Bmp4	5'-CAGGAGATCAGCCTGCAGTAC-3'	5'-TGCTGAGGTTGAAGACGAAGC-3'	60°C
Sema3a	5'-TGGAGTAGAGAATAGCAGCAC-3'	5'-TGTCCGGATCATTCGATCATC-3'	60°C
Sema3d	5'-CTGCCAGAGACCCATACTGTG-3'	5'-GCAGTTTCATGACTAATGCTG-3'	60°C
Sema3e	5'-GCGAGCCCATGAAACTAAGAAG-3'	5'-ATGCTGTGTTCCACTGTCTGAC-3'	60°C
Sema3f	5'-ACCCATCAAGATGATGACCATC-3'	5'-CAGGCTTCTCCATACACGTCA-3'	60°C

Table S2. Fusion of the dorsal aortae in unmanipulated quail and chick embryos compared with somite position

Quail		Chick	
Stage	Somite position at fusion	Stage	Somite position at fusion
12	No fusion (n=14)	12	No fusion (n=15)
13	10.7 (n=12)	13	10.5 (n=13)
14	13.6 (n=10)	14	13.2 (n=7)
15	16.2 (n=6)	15	15.9 (n=8)

Table S3. Site of Chordin downregulation in the notochord compared with the site of dorsal aortae fusion and somite position in chick

Stage	Somite position at fusion	Somite position at undetectable Chordin	Difference	Number
12	No fusion			$n=5$
13	10.5 (±1.21)	15.1 (±1.04)	4.9 (±1.30)	$n=11$
14	13.2 (±0.52)	18.3 (±0.52)	5.3 (±0.76)	$n=7$

Table S4. Fusion of the dorsal aortae in quail embryos in ovo compared with New cultured sibling embryos

Stage	Somite position at fusion in New culture	Somite position at fusion in ovo
11	No fusion (*n*=13)	No fusion
12	9.3 (*n*=14)	No fusion
13	11.5 (*n*=16)	10.5 (*n*=13)
14	13.7 (*n*=3)	13.2 (*n*=7)